PERGAMON

Deep-Sea Research I 49 (2002) 735–749

DEEP-SEA RESEARCH
PART I

www.elsevier.com/locate/dsr

Mesoscale distribution of zooplankton in the Sub-Antarctic Frontal system in the Indian part of the Southern Ocean: a comparison between optical plankton counter and net sampling

J.Ph. Labat[a,*], P. Mayzaud[a], S. Dallot[a], A. Errhif[a], S. Razouls[b], S. Sabini[a]

[a] *Océanographie Biochimique et Ecologie, Laboratoire d'Océanographie de Villefranche sur mer (LOV), UPMC-INSU-CNRS, Paris VI, Maitre de Conferences, Observatoire Oceanologique, BP. 28, 06234 Villefranche sur mer, France*

[b] *Equipe d'Océanographie biologique, UPMC-INSU-CNRS, Laboratoire Arago, 66650 Banyuls-sur-mer, France*

Received 23 April 2001; received in revised form 23 October 2001; accepted 5 November 2001

Abstract

(*Antartic Research (ANTARES) IV Cruise, January–February* 1999). Distribution of zooplankton biovolume/biomass in the Sub-Antarctic Frontal system is described for the Indian Ocean sector, northwest of Kerguelen Islands, with a comparison of two types of sampling techniques: WP2 net and optical plankton counter (OPC). During the *ANTARES IV* Cruise (January–February 1999), three zones were sampled: the Polar Frontal Zone (PFZ), south of the Sub-Antarctic Front; the Frontal Zone between the Sub-Tropical Front; and the Agulhas Front and the Sub-Tropical Zone, north of the main stream of the Agulhas Return Current. Copepods were the dominant group in all net samples regardless of the area considered. Maximum values were recorded in the PFZ with both net catches and OPC. A strong contrast in terms of population structure and biomass was observed between the zone south of the Sub-Antarctic Front and the zones to the north. The patterns of the zooplankton biovolume distribution by size confirmed this relationship. Biovolume 2D maps showed in this south area a more patchy distribution than in the other areas where a vertical gradient dominated. The OPC data are in fair agreement with net sample data and are spatially heterogenous in both size structure and biomass.

Keywords: Southern Ocean; Zooplankton; Biomass; Size distribution; Spatial variation; Optical plankton counter; Sub-Antarctic Frontal system

1. Introduction

Zooplankton play a key role in food web dynamics and represent the main food source for many important fish stocks. Traditionally, net tows are used to study zooplankton communities, but they are often poorly suited when there is spatial heterogeneity and render difficult integration of data at different scales. This is particularly true when measurements of zooplankton biomass are expected to show patchiness, such as in areas with contrasting hydrologic structures. The use of

*Corresponding author. Tel.: +33-04-9376-3845; fax: +33-04-9376-3893.

E-mail address: jean-philippe.labat@obs-vlfr.fr (J.Ph. Labat).

0967-0637/02/$ - see front matter
PII: S0967-0637(01)00076-0

optical plankton counter (OPC) introduced by Herman (1988, 1992) represents an alternative to characterize, at different scales, abundance and size distribution of zooplankton. OPC is a powerful tool permitting description of size distribution of zooplankton at both large and small scales (Herman et al., 1993; Huntley et al., 1995; Kato et al., 1997; Mullin and Cass-Calay, 1997; Osgood and Checkley, 1997; Currie et al., 1998; Wieland et al., 1997; Grant et al., 2000; Huntley et al., 2000). Knowledge of changes in size structure of plankton communities has long been recognized as essential to understanding of population dynamics at the mesoscale (Sheldon et al., 1972; Vidal and Whitledge, 1982).

Here we present data from the Antarctic Research (*ANTARES*) *IV* Cruise (January–February 1999). *ANTARES* is the French contribution to Southern Ocean-Joint Global Ocean Flux Study (SO-JGOFS).

Zooplankton distributions were considered in a study area characterized by a strong horizontal temperature and salinity gradient (Park and Gamberoni, 1997) close to both Sub-Antarctic and Sub-Tropical Fronts (STFs) in the Indian Ocean (Nagata et al., 1988). We compare the continuous record of the distribution of zooplankton biovolume/biomass in the different water masses and describe the characteristics of the zooplankton population structure in these areas of very contrasting hydrological structures.

2. Material and methods

Zooplankton samples were collected in three main hydrological domains, chosen after a preliminary mesoscale survey of the area:

- Station 3 area, was located in the Polar Frontal Zone (PFZ), south of the Sub-Antarctic Front.
- Station 7 area was located in the Frontal Zone between the STF and the Agulhas Front (AF).
- Station 8 area was located in the Sub-Tropical Zone (STZ), north of the main stream of the "Agulhas Return Current" (sometimes called "South Indian Ocean Current") (Park and Gamberoni, 1997).

During net sampling, a Lagrangian approach was used, with the ship following a drifting buoy for the duration of the stations. Fig. 1 shows the position of net hauls and OPC lines.

2.1. Net sampling

Zooplankton were collected at night with a triple WP2 net ($0.25\,m^2$ surface aperture and 200 μm mesh size). Vertical hauls were made from 200 m to the surface. One net was used for biomass measurement and another one for taxonomic description and enumeration.

Biomass samples were filtered on 200 μm preweighed netting and rinsed with ammonium formate. The material was immediately frozen at −20°C on board. Within 3 months, all samples were oven dried (48 h at 60°) at the laboratory and weighed. Total weight is expressed in milligram of dry weight per cubic meter, DW $mg\,m^{-3}$.

Taxonomic samples were preserved immediately after the catch, with 5% buffered formaldehyde.

2.2. Net sample treatments

Species determinations, enumerations and biovolume estimates were made with a binocular microscope coupled to an image analysis system. An equivalent spherical diameter (ESD) size distribution was constructed for each net sample. Sub-samples of 200–400 individuals (with a Motoda box splitter) were used to measure the ESD of each individual with a Visiolab 1000 system (Biocom). ESD of an organism was defined as the diameter of the sphere that has an identical projected surface.

Sample biovolume (SBV) of each sample was computed from the individual ESD measurement:

$$\mathrm{SBV} = k\left[\sum_{i=1}^{n}\frac{\pi}{6}(\mathrm{ESD}_i)^3\right],$$

where k is the sub-sample ratio, n the number of individuals, and ESD_i the ESD of the ith individual.

For each sample, the value of SBV can be associated with a value of total biomass derived from the corresponding net. It was then possible to

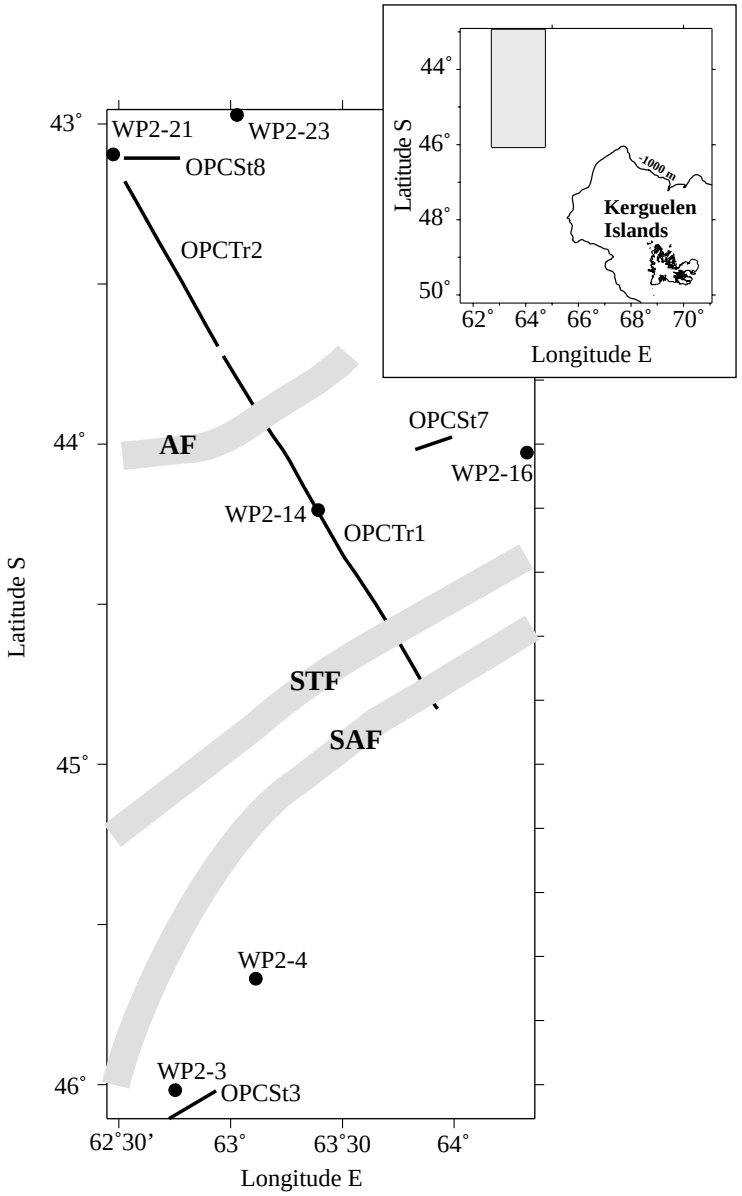

Fig. 1. Positions of stations (calibration hauls) and transect of OPC records during the *ANTARES IV* Cruise. AF: Agulhas Front, STF: Sub-Tropical Front, SAF: Sub-Antarctic Front. Fronts are positioned from the hydrological data.

compute a biovolume-to-biomass conversion (BBC) function. Because of the limited number of net hauls per station, it was not possible to compute area-specific functions. As an alternative, we chose to compute a global all-station relationship.

2.3. OPC records

The in situ OPC (Herman, 1988, 1992) is capable of counting and sizing of particles from 0.25 mm to >1 cm. The design, calibration and mode of operation of the OPC has been fully

described by Herman (1988, 1992). Briefly, the OPC consists of a flow-through tunnel, and particles passing through the tunnel cross a rectangular light beam, the attenuation of which is proportional to the size of the particle. OPC employs a narrow light beam of 4 mm width, 20 mm height and 220 mm length. Each particle going through this beam is viewed as a projected surface. Thus the digital size recorded when a particle passes through can be converted to a diameter, which is the diameter of a sphere blocking the same amount of light as the particle (ESD). Output from the OPC in an integer varying from 0 to 4095. The OPC we used was the -1T model. It was mounted on a Batfish vehicle with a CTD sensor (Seabird SB25) and towed at a speed between 7 and 9 knots in a saw-tooth undulating pattern cycling between the surface and 70 or 200 m depth. The position of the ship was recorded from a GPS system. The distance covered was computed from the position data. The volume of water passing the OPC was estimated from this distance and the tunnel dimensions.

In each sampling area, a short OPC transect (around 10 n.m.) was achieved in connection with two calibration hauls during the night period. A two part, long transect of 110 nautical miles (n.m.): OPC tr1 and OPC tr2, crossed the general hydrologic structure from the PFZ to the STZ. Physical parameters were recorded during both sections, but for technical reasons plankton size data were recorded only during OPC tr2. OPC tr2 was also done during the night period.

At station 3, the depth range covered by the oscillation was between the surface and 70 m. For the two other stations (7 and 8) the Batfish oscillated between the surface and 200 m depth. For stations 3 and 8, the same transect was covered twice back and forth.

OPC data acquisition software was used to convert signals from the underwater unit into standard OPC text files. These raw data were transformed using software developed locally (TADO 4.2; Labat unpublished). Size count data and physical measurements were pooled by spatial unit cells delimited by chosen intervals for horizontal and vertical dimensions. For each unit cell the means of physical parameters were computed and the corresponding size distribution recorded. Size distribution can be expressed either as number per size class or as volume per size class. The volume was calculated as parts per billion or $mm^3\,m^{-3}$. The estimated biovolume by size class represented a proxy of the biomass as a function of size. All these unit cells are spatially localized by a depth and a distance from starting point of the transect. To analyze the global size distribution of the transect, a preliminary approach was done with 255 size classes of 50 μm interval ranging from 0.250 to 13 mm. Then a second estimate was computed with size classes corresponding to the homogeneous groupings observed in the preliminary analysis.

The maps of biovolume were interpolated by a triangulation method with linear interpolation. This method was used because it is an exact interpolator where data are honored very closely and no grid nodes were computed outside of the range of data. A grid dimension of 40×30 was used. Computations were made using Surfer 7.0 Software.

2.4. Correspondence between ESD view by the OPC and ESD view by the Visiolab

To verify correspondence between the different estimates of ESD by OPC and by image analysis, an intercalibration was performed. A moving averaged smoothing was used to avoid the influence of local variations. We used correspondences between easily distinguishable points, e.g. maxima and minima of distribution up to an ESD of 2 mm, beyond which data became too irregular to be meaningful. Small shifts between both estimates were corrected with a linear function: $ESD_{opc} = (0.86 \pm 0.07)ESD_{visio} - (0.04 \pm 0.11), (n = 12, r = 0.97, p < 0.01)$.

3. Results

Table 1 gives the characteristics of the net sampling and the Table 2 the characteristics of the OPC transect.

Table 1
WP2 net sampling and corresponding biovolume and biomass values

St. no.	Date	Net label	Type, depth (m)	N (m^{-3})	Biovolume ($mm^3\,m^{-3}$)	Biomass ($DW\,mg\,m^{-3}$)
3	19/01/1999	WP2-3	Vertical, 0–200	1036	151.2	64.1
3	21/01/1999	WP2-4	Vertical, 0–200	232	162.2	66.4
7	06/02/1999	WP2-14	Vertical, 0–200	131	55.8	10.2
7	09/02/1999	WP2-16	Vertical, 0–200	299	80.0	12.7
8	12/02/1999	WP2-21	Vertical, 0–200	246	57.4	18.2
8	15/02/1999	WP2-23	Vertical, 0–200	520	138.4	30.0

Symbols: Dw = dry weight; N = number of individuals per unit volume.

Table 2
Characteristics of OPC samples

St. no.	Date	OPC label	Depth (m)	Transect length (n.m.)	Sampled volume (m^3)	N (m^{-3})	Mean biovolume ($m^3\,m^{-3}$) 0–70 m	Mean biovolume ($m^3\,m^{-3}$) 0–200 m	Computed biomass ($DW\,mg\,m^{-3}$) 0–70 m	Computed biomass ($DW\,mg\,m^{-3}$) 0–200 m
3	18/01/99	OPC st3	0–70	10 FB	158.1	1597	228.9	143.4[a]	90.88	50.53[a]
7	10/02/99	OPC st7	0–200	6 F	69.0	558	118.7	73.4	38.88	17.51
8	13/02/99	OPC st8	0–200	10 FB	188.2	519	89.3	52.6	25.01	7.69
Tr2	12/02/99	OPC tr2	0–200	35 F	323.8	334	76.2	51.2	18.83	7.03

[a] Values back-calculated with the ratio (0.62) to compensate for depth range differences (see text).
F: One way transect, FB: forward and backward transect. Biomasses were computed from the biovolumes.

3.1. Hydrographic conditions

The depth profiles of temperature along the transect OPCTr are shown in Fig. 2. The positions of the Sub-Antarctic Front (SAF) ($T = 6^\circ$ at 200 m), the STF (10° at 200 m) and the AF (14° at 200 m) were obvious. These hydrological structures delimited the PFZ south of the SAF, the Frontal Zone between the SAF and the AF and the STZ north to the STF, associated with the Agulhas Return Current (ARC) north of the AF (Park and Gamberoni, 1997).

3.2. Mean biovolume and biomass

Highest biovolumes (151.2 and 162.2 $mm^3\,m^{-3}$) and biomass (64.1 and 66.4 $DW\,mg\,m^{-3}$) were recorded at station 3, in the PFZ (Table 1). In the other zones, both biomass and volumes were higher in the ARC (biovolumes: 57.4 and 138.4 $mm^3\,m^{-3}$; biomass: 18.2 and 30.0 $DW\,mg\,m^{-3}$) than in the Frontal Zone (biovolumes: 55.8 and 80.0 $mm^3\,m^{-3}$; biomass: 10.2 and 12.7 $DW\,mg\,m^{-3}$). Both descriptors were significatively correlated ($n = 6$, Spearman $r = 0.942$, probability < 0.01), and a linear regression was fitted to define a BBC function (biomass = (0.47 ± 0.11)biovolume $-(17.1 \pm 12.3)$, biomass in DW mg, biovolume in mm^3, $p < 0.01$).

At station 3, the mean biovolume estimated by the OPC was high, 228.9 $mm^3\,m^{-3}$, for a depth range limited to 0–70 m. For comparison with net data, a correction factor must be computed to account for the difference in depth range between the two sampling gears (from the biovolume ratio between 0–200 and 0–70 m recorded in the three other OPC records, a factor of 0.62 can be used). The 0–200 m corrected biovolume was 143.4 $mm^3\,m^{-3}$, a value similar to that derived from net sampling (151.2–162.2 $mm^3\,m^{-3}$). At station 7, the biovolume from the two nets WP2-14 and WP2-16 were different, 55.89 and 80.0 $mm^3\,m^{-3}$, respectively, but the range observed appears to agree with the mean biovolume

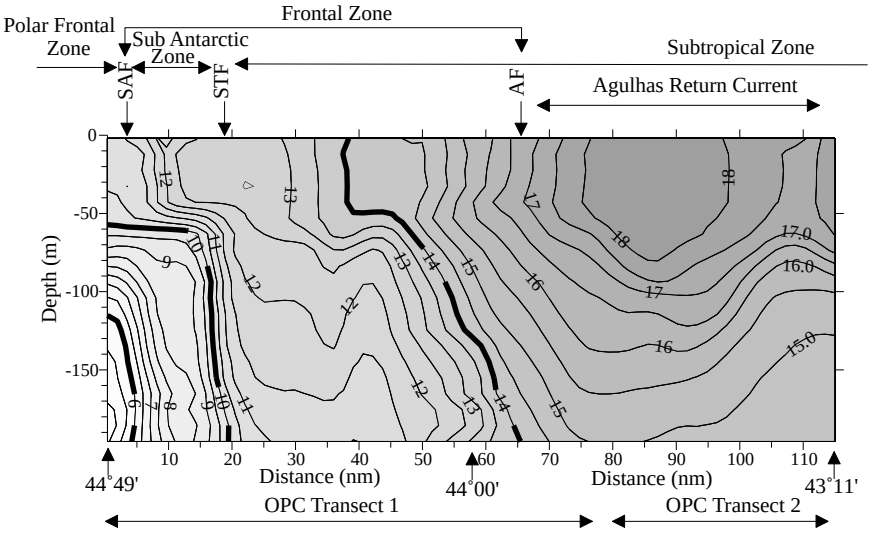

Fig. 2. Temperature profile along the OPC tr1 and OPC tr2 transects, contour levels are given at 0.5°C intervals. SAF: Sub-Antarctic Front (6°C at −200 m), STF: Sub-Tropical front (10°C at −200 m), AF: Agulhas Front (14°C at −200 m). Zone limits from Park and Gamberoni (1997).

computed from the corresponding OPC transect, 73.3 $mm^3 m^{-3}$. In the station 8/transect 2 area, the difference in biovolume between the two net hauls was even greater (57.4 and 138.4 $mm^3 m^{-3}$), and both were larger than the mean biovolumes computed from the OPC data at OPC st8 and OPC tr2 (52.62 and 51.2 $mm^3 m^{-3}$, respectively).

3.3. Taxonomic composition

Zooplankton taxonomic composition and ESD of the main species is reported in Table 3. Copepods were the dominant group in all net samples regardless of the area considered.

3.4. Number by size classes in the OPC data

The size distribution showed one peak with the maximum number of individuals in the size class 0.35 mm (Fig. 3). OPC st3 illustrated the higher abundance in the Sub-Antarctic Zone compared to the other survey lines with enhanced difference in the 1–2 mm size range. OPC st8 and OPC tr2 corresponded to similar geographical zones and showed minimum values with almost identical size profiles.

3.5. Distribution of biovolume by size class

Station 3: Size distribution of biovolume showed important differences on the one hand between the two nets samples and on the other hand between the net samples and the OPC (Fig. 4A). Net sample WP2-3 and OPC presented a size profile with a mode around 0.5 mm not seen in the WP2-4 net sample. A comparison with the size characteristics and abundance (Table 3), suggested a major contribution of the following species: *Oithona* spp., *Clausocalanus* spp. and *Ctenocalanus citer*. Because the densities observed in the larger size categories are relatively similar, the difference between WP2-3 and WP2-4 samples can be related to the presence of small individuals belonging to this taxonomic group in WP2-3. The similarity in total volume (151.2 and 162.2 $mm^3 m^{-3}$) confirmed that animal concentrations decrease with increasing size (1036 n. $m.^{-3}$ in WP2-3 and 232 n. $m.^{-3}$ in WP2-4).

In the 1–2 mm range, WP2-3 showed a mode around 1.25 mm ESD, which is masked by a broader peak around 1.6 mm for WP2-4 (Fig. 4A). This size range corresponds to *Calanus simillimus* and *Neocalanus gracilis* as major contributors. Interestingly, within this size range, the size

Table 3
Main taxa found in the calibration nets

St. no.	Net	N (m^{-3})	Dominant taxa	% N	ESD mean (std)
3	3	1036.8	*Ctenocalanus citer*	51.6	0.60*
			Clausocalanus spp.	28.5	0.63 (0.07)
			Oïthona spp.	9.8	0.34 (0.01)
			Ostracoda	2.7	0.72 (0.08)
			Euphausiid larvea	1.2	2. 2 (1.3)
			Calanus simillimus	1.0	1.52 (0.10)
3	4	232.8	*Oithona* spp.	19.5	0.34 (0.01)
			Clausocalanus spp.	19.0	0.64 (0.07)
			Ostracoda	12.5	0.68 (0.37)
			Calanus simillimus	7.3	1.52 (0.10)
			Neocalanus gracilis	5.6	1.25*
			Gasteropoda	5.5	0.60 (0.45)
			Metridia lucens	5.2	1.09 (0.09)
			Ctenocalanus citer	4.1	0.60*
			Euphausiid larvae	2.8	2.2 (1.3)
7	14	131.1	*Clausocalanus* spp.	49.1	0.64 (0.07)
			Pleurommama borealis	18.5	0.79 (0.12)
			Oithona spp.	7.1	0.34 (0.01)
			Metridia lucens	7.0	1.09 (0.09)
			Mecynocera clausi	5.9	0.5*
			Chaetognatha	2.7	1.24 (0.48)
			Pleurommama spp.	2.1	—
			Ostracoda	1.8	1.47 (0.40)
7	16	299.5	*Clausocalanus* spp.	44.3	0.64 (0.07)
			Metridia lucens (C VI)	33.4	1.09 (0.09)
			Pleurommama borealis	12.1	0.79 (0.12)
			Oncaea spp.	1.9	—
			Oithona spp.	1.5	0.34 (0.01)
			Pleurommama spp.	1.4	—
			Ostracoda	1.3	1.47 (0.40)
8	21	143.2	*Pleurommama borealis*	43.1	0.79 (0.12)
			Clausocalanus spp.	28.6	0.64 (0.07)
			Peurommama spp. *(copepodite)*	7.2	—
			Pleurommama abdominalis	6.9	1.69 (0.29)
			Scolecithricella ovata	3.1	1.0*
8	23	590.4	*Clausocalanus* spp.	47.1	0.64 (0.07)
			Pleurommama borealis	24.3	0.79 (0.12)
			Oithona spp.	2.4	0.34 (0.01)
			Neogracilis gracilis	3.8	1.25*
			Pleurommama abdominalis	1.5	1.69 (0.29)

N (m^{-3}): total number by cubic meter, %: abundance in percentage. ESD: equivalent spherical diameters in mm, mean and standard deviation. ESD labeled by * are computed from size value of Razouls (1995, 1996).

spectrum computed from the OPC data was similar to the spectrum of sum of both nets. Around 2 mm the WP2-3 sample showed an important contribution, which is likely related to euphausiid larvae, more abundant in WP2-3 than in WP2-4. The lack of biomass in this size range in

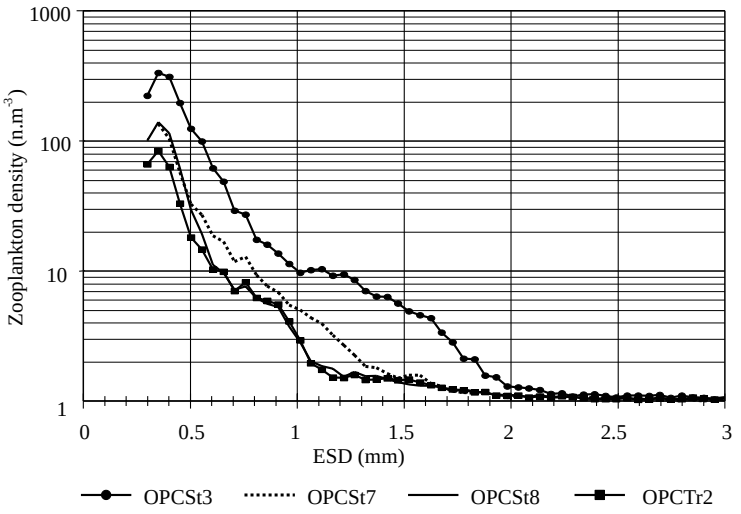

Fig. 3. Zooplankton density (n. m.^{3}) changes by size using a 50 μm size class interval, recorded by the OPC for the 4 data sets. A logarithmic scale is used and the value transformed in $(n+1)$.

the OPC profile could be linked to the depth of sampling as it was limited to 70 m.

Station 7: The size profiles presented in Fig. 4B showed that the patterns of size distribution were reasonably close between nets, and, if we exclude the smaller size classes (<0.6 mm), between nets and OPC. The difference in total biovolume between nets (55.8 and 80.0 $mm^3 m^{-3}$ for WP2-14 and WP2-16, respectively) can be attributed to the larger biovolume in the 1 mm range for the WP2-16 haul. The intermediate biovolumes computed from the OPC line is indicative of a spatial integration of local patchiness. From Table 3, it can be infered that *Oithona* spp. composed most of the peak around 0.4 mm, *Clausocalanus* spp. and *Pleurommama borealis* the 0.7 mm size range, *Metridia lucens* the peak around 1.1 mm, and *Ostracoda* and *Pleurommama* species *(P. robusta, P. abdominalis and P. xiphias)* the peak around 1.6 mm.

Station 8 *and transect* 2: The general pattern of biovolume per size class is reasonably similar but, as already seen at station 7, varied strongly in intensity (Fig. 4C). Except in the smaller size range (<0.6 μm) biovolumes measured from net hauls were larger than computed from OPC data. The population sampled by the two sampling device recorded two modes in size, 0.8 and 1.7 mm. Oithonidae copepods are the main components of the smaller size range, and *Clausocalanus* spp, *Pleurommama borealis*, copepodites of larger *Pleurommama* species and *Scolecithricella ovata* constituted the peak around 0.8 mm. Between 1.2 and 2.4 mm the population is likely dominated by *Neogracilis gracilis* and *Pleurommama abdominalis*.

3.6. Spatial distribution of zooplankton biovolume per size class

From the above analyses size coherent groupings were defined. The maps of zooplankton biovolume (Figs. 5–8) illustrate the spatial variability in both vertical and horizontal dimensions of each coherent size group.

Station 3: The depth distribution of biovolume is presented over the depth range actually sampled by the OPC. The overall size distribution was divided into two size categories, corresponding to Fig. 4A, i.e., 0.25–1.0 and 1.0–2.1 mm. These two size groups represented, respectively, 35.4% and 47.4% of the biovolume recorded by the OPC. Strong heterogeneity can be seen for both size groups over the two spatial dimensions, depth and distance (Fig. 5). The contrast in both dimensions was stronger for the larger size group. For the

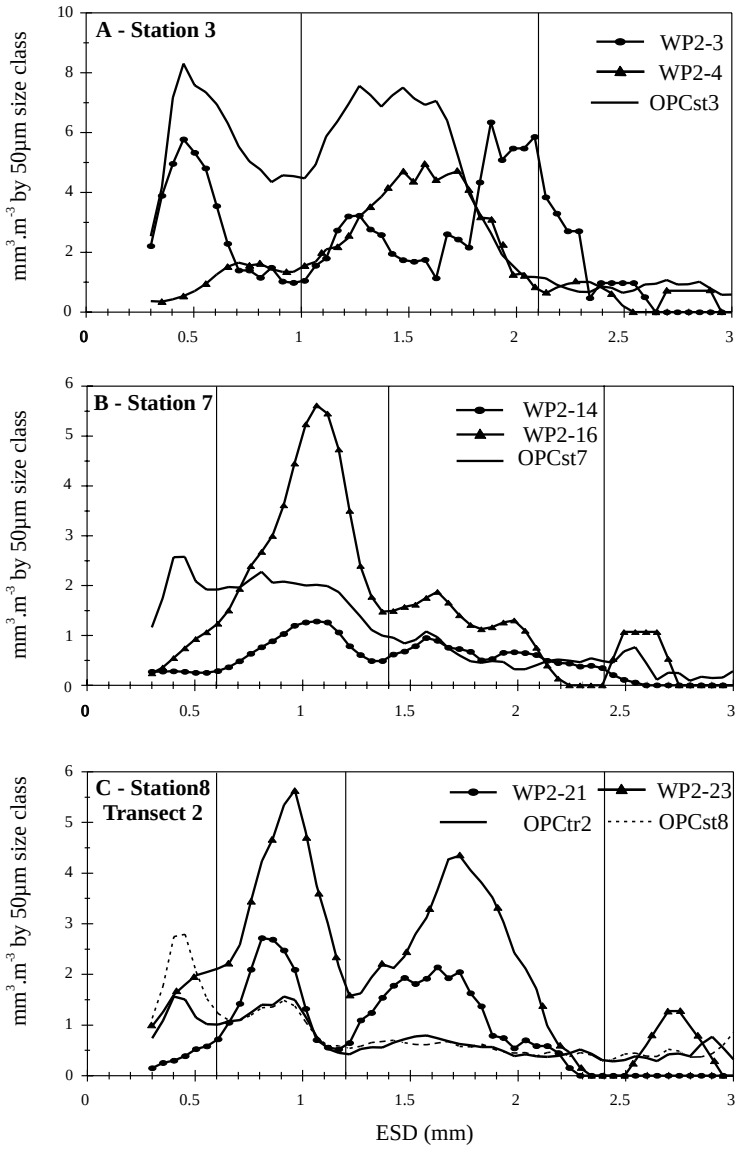

Fig. 4. Volume ($mm^3\,m^{-3}$) distribution by size using a 50 µm class interval for both net samples and OPC records. (A) Station 3 area, (B) station 7 area, (C) station 8 area and transect 2. Vertical lines indicate limits of coherent size groupings used.

0.25–1.0 mm set, maximum density occurred between 40 and 65 m but over the first 4 mile of the transect. A sub-surface continuous layer of high biovolume appears characteristic of the area. For the larger size range (1.0–2.1 mm) the map showed a patch of maximum abundance centered around 15 m depth with very high biovolume exceeding $650\,mm^3\,m^{-3}$. The strata between the surface and the maximum layer of zooplankton showed volume exceeding $200\,mm^3\,m^{-3}$. The size group above 2.1 mm (not shown) made up 17.2% of the total biovolume and an extremely patchy distribution.

Station 7: The size distribution was divided into three size classes, 0.25–0.60, 0.6–1.4 and 1.4–2.5 mm (corresponding, respectively, to 19.0%, 38.2% and 16.7% of the total biovolume). The

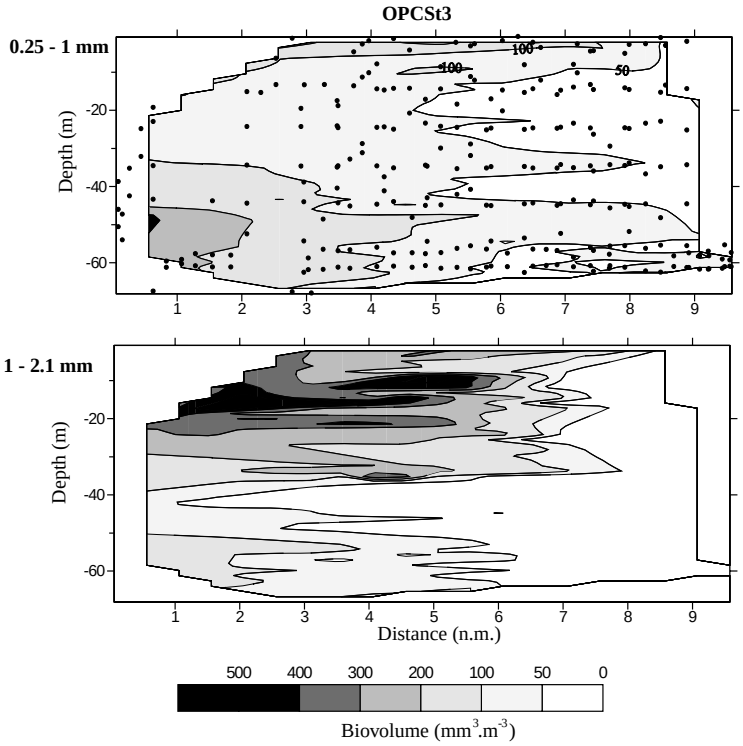

Fig. 5. Spatial distribution of the biovolume distributions ($mm^3\,m^{-3}$) for the two size groups at station 3. (A) 0.25–1.0 mm, (B) 1.0–2.1 mm. In graph A, dots indicate position of the values used for interpolation.

spatial and vertical distribution of the three size groups followed a very similar pattern (Fig. 6): higher density of biovolume near the surface, rapid decrease down to 20 m, and slowly changing volumes from 20 to 70 m. Sizes >2.4 mm (not shown) represented 25.7% of the biovolume recorded by the OPC.

Station 8 *and transect* 2: Size distribution has been regrouped into three size categories: 0.25–0.6, 0.6–1.2 and 1.2–2.4 mm. They represented, respectively, 24.4%, 21.6% and 23.1% of the total biovolume for station 8 and 15.7%, 24.2% and 24.7% for transect 2. Along transect 2 (Fig. 7), maximum densities were observed for the 0.6–1.2 mm size group, with a marked vertical and horizontal structure. A high-density zone was located in the central part of the warmest water of the ARC (see Fig. 2) between 10 and 20 mile from the transect starting point. In the terminal part of the transect between 28 and 34 mile, out of the main stream of the ARC, a patch of biovolume around $30\,mm^3\,m^{-3}$ move down to 100 m. The size group between 1.2 and 2.4 mm has a similar but more patchy distribution in the vertical dimension. Smaller size individuals (0.25–0.60 mm) showed relatively small biovolumes limited to the first 70 m. At station 8 (Fig. 8), the OPC distributions for the same size categories also showed a vertically structured pattern. The main difference was the presence of a deep layer of small size organisms in the 0.25–0.6 mm range, with values $>10\,mm^3\,m^{-3}$ below 150 m.

3.7. Estimation of the biomasses from the OPC data

From the biovolumes recorded by the OPC and the BBC function, a biomass was estimated for the OPC transects. Biomass estimates showed (Table 2) higher values for the Polar Front Zone ($90.9\,DW\,mg\,m^{-3}$ between 0 and 70 m and $50.5\,DW\,mg\,m^{-3}$ between 0 and 200 m) than for

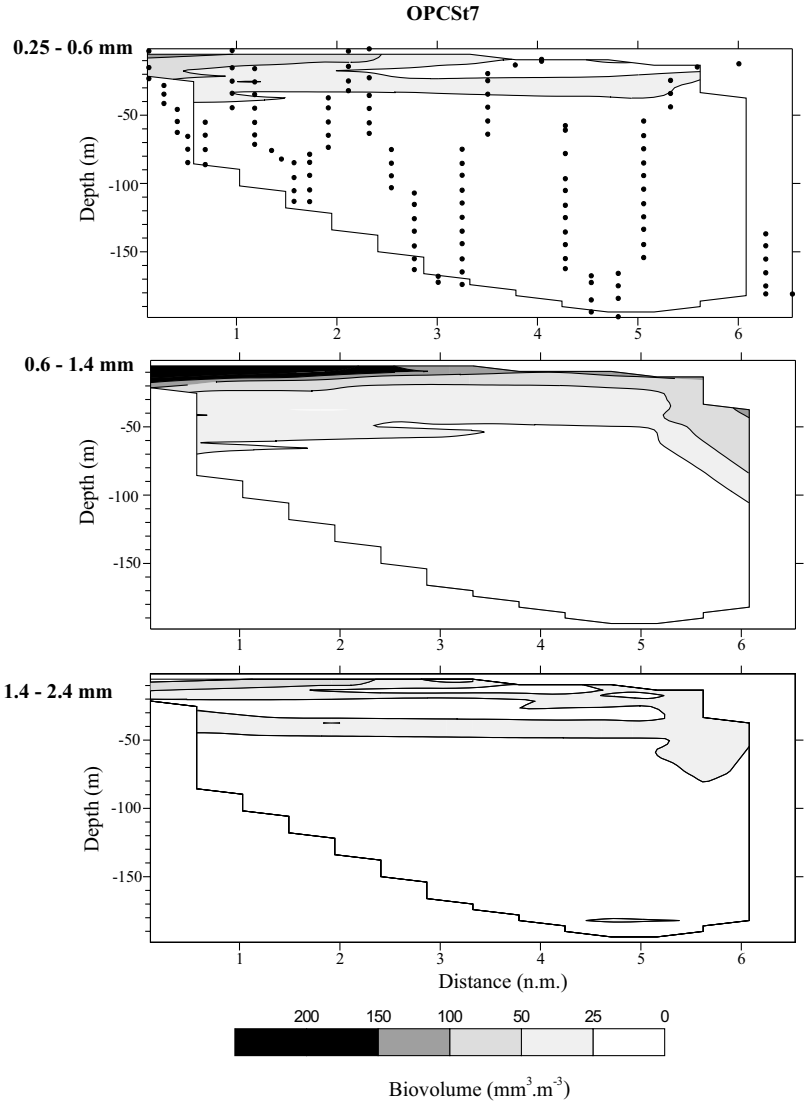

Fig. 6. Spatial distribution of the biovolume distributions ($mm^3\,m^{-3}$) for the three size groups at station 7. (A) 0.25–0.60 mm, (B) 0.6–1.4 mm, (C) 1.4–2.4 mm. In graph A, dots indicate position of the values used for interpolation.

the two other zones (18.8–38.95 DW mg m^{-3} between 0 and 70 m and 7.0–17.55 DW mg m^{-3} between 0 and 200 m).

4. Discussion

The global zooplankton perception by the OPC may present technical limitations, particularly with regard to translucent organisms and coincident counts. The biovolume of transparent organisms may be misread by the device, leading to an increased bias in size measurements as such organisms become abundant. However, in this study, transparent organisms were relatively poorly represented in the catches which were mainly made up of copepods and other crustaceans. Another kind of bias may arise when two or

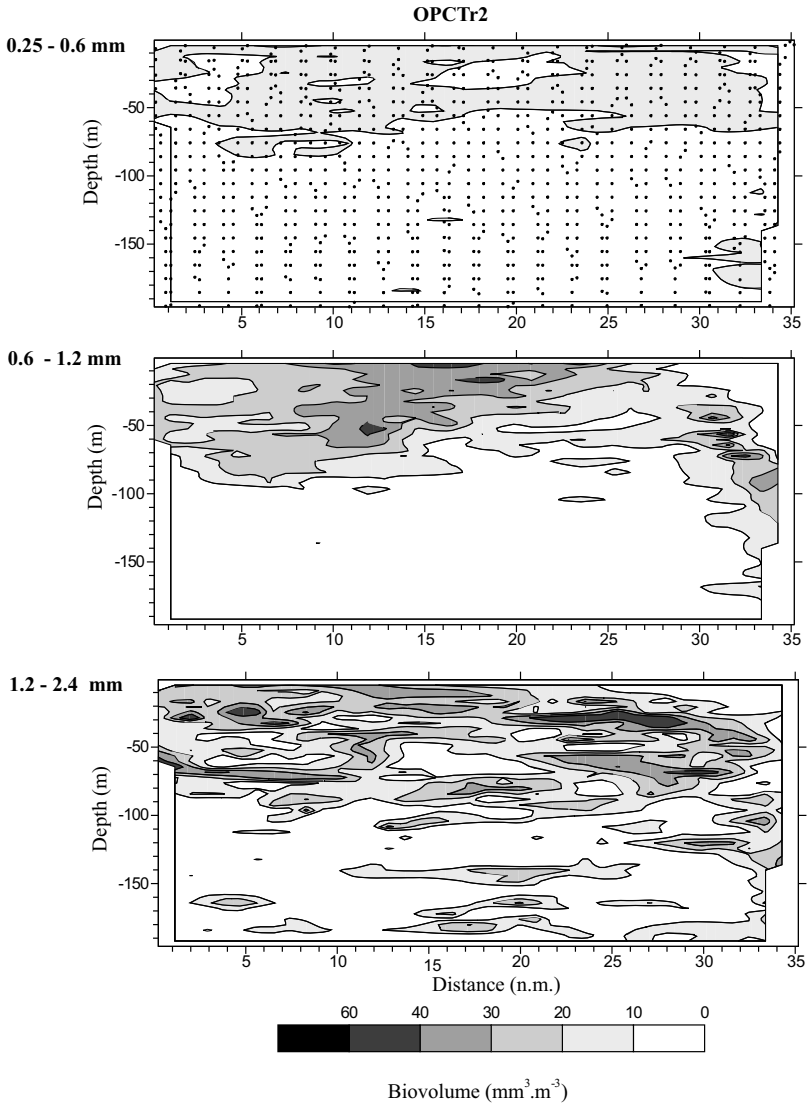

Fig. 7. Spatial distribution of the biovolume distributions ($mm^3\,m^{-3}$) for the three size groups for transect 2. (A) 0.25–0.60 mm, (B) 0.6–1.2 mm, (C) 1.2–2.4 mm. In graph A, dots indicate position of the values used for interpolation.

more particles pass simultaneously through the detection beam and are thereby not resolved as separate objects. During the cruise, counts per second were <50 for the richest zone. This was far below the minimum level at which coincidence is considered to become significant (Herman, 1992; Sprules et al., 1998; Heath et al., 1999).

4.1. Comparison between sampling methods and variability in population structure

The OPC has been used to obtain data permitting description of zooplankton spatial distribution (Huntley et al., 1995; Stockwell and Sprules, 1995; Osgood and Checkley, 1997; Kato et al., 1997; Grant et al., 2000). Comparisons of OPC

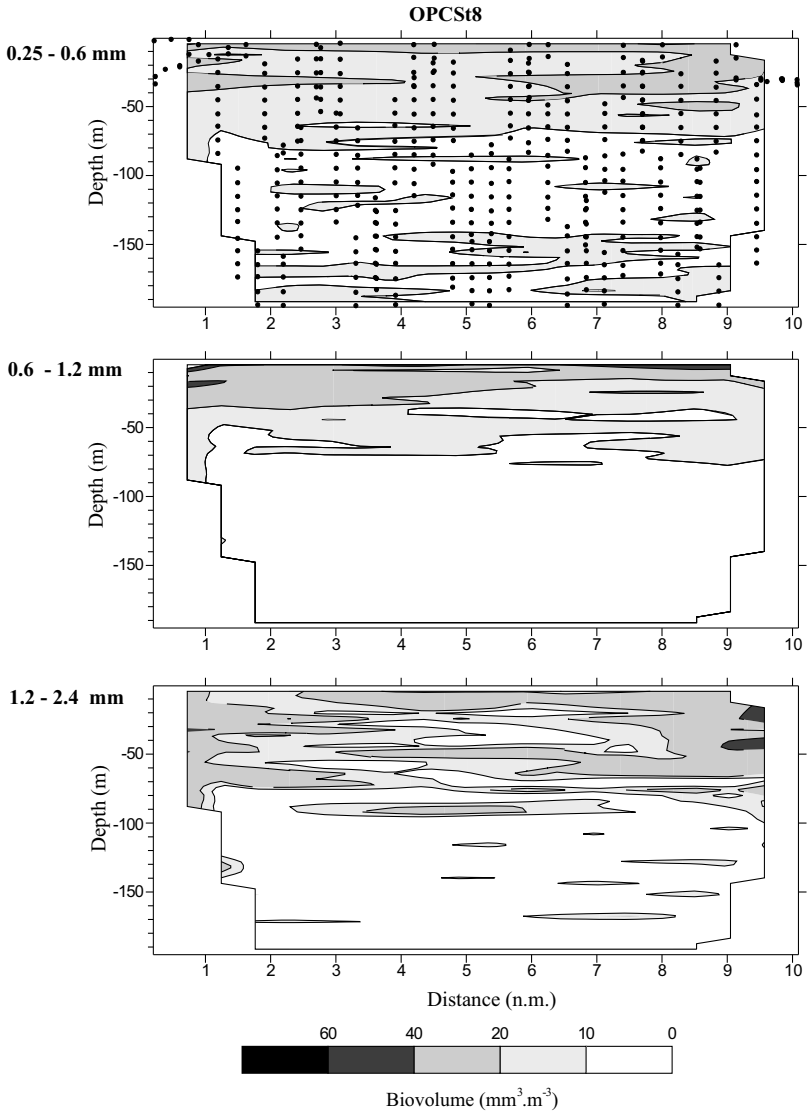

Fig. 8. Spatial distribution of the biovolume distributions ($mm^3\,m^{-3}$) for three size groups at station 8. (A) 0.25–0.60 mm, (B) 0.6–1.2 mm, (C) 1.2–2.4 mm. In graph A, dots indicate position of the values used for interpolation.

with other sampling gear such as nets have yielded somewhat contradictory results (Sameoto et al., 1990; Sprules et al., 1998; Grant et al., 2000). In the present study, the computed OPC biovolumes are close but not identical to the net estimate of the same biovolumes. OPC values fell between net estimates at station 7 and were somewhat lower for stations 3 and 8. The difference in the scale sample by the two methods probably explains such divergence. The pattern of zooplankton size distribution obtained from net samples is generally sharper than with the OPC. The broader OPC distribution reflects the variability in animal orientation when passing through the light beam (Sprules et al., 1998). Part of the difference may also originate from the different spatial scales of sampling: nets are vertical snapshots whereas OPC integrates larger spatial domains. The distribution

recorded at station 3 provides a good example with a strong divergence in the size distibution between the two nets, which agree with the OPC distribution when the mean of the two nets is considered. This phenomenon is particularly obvious at this station where the zooplankton distribution is patchiest in both dimensions. Another key feature of the OPC records is the better representation of the smaller sizes of zooplankton with a constant mode below 0.5 mm, corresponding mainly to the group of small Oithonidae.

4.2. OPC biomass estimate

Biovolume can be used as a proxy of biomass (Mullin and Cass-Calay, 1997). However, actual biomass is often needed, and conversion factors between biovolume ($mm^3 m^{-3}$) and biomass ($DW mg m^{-3}$) should be defined. In the present study, we used a general BBC function computed from the pooled net measurements of all areas. The results showed some divergence with the net dry weight measurements within one zone. The high net derived biomass within the PFZ was also recorded by the OPC but the larger biomass measured by nets at station 8 compared to station 7 was not detected by the OPC. This could be explained either by the difference in spatial integration or by the possibility that the BBC function varied with local plankton composition. Unfortunately, the number of calibration nets available was too small to test statistically the inter-zone difference of the BBC function.

4.3. Distribution of the zooplankton in the frontal system

A strong contrast in terms of population structure and biomass was observed between the areas south of the SAF and the other domains north of this limit. *Calanus simillimus* and *Ctenocalanus citer* characterized the Sub-Antarctic populations, while *Pleuromma borealis* and *P. abdominalis* characterized those north of the STF. A similar pattern has been reported by Grachev (1991) (cited in Pakhomov et al., 2000) by Barange et al. (1998) and by Pakhomov et al. (2000) for the Atlantic Sub-Antarctic Frontal Zone, where *C. simillimus* dominated the biomass in the SAZ, and *Pleuromma* spp. dominated in the STZ (Sub-Tropical Convergence (STC) for Barange et al., 1998; and Pakhomov et al., 2000) north of the STF. The same opposition between north and south of the SAF emerged from the size distribution by number and by volume irrespective of the sampling system considered. Station 3 in the PFZ showed contrasted profiles compared to the other station and area (station 7—FZ and station 8—STZ).

In terms of biomass, maximum values were recorded in the PFZ both by net catches and OPC records. The mean values of biomass observed for the same season by Pakhomov et al. (2000) in the SAF area are in excellent agreement with the present data, i.e., 47.2 $DW mg m^{-3}$ (21.6–91.5) for the PFZ; 6.52 $DW mg m^{-3}$ (2.4–9.9) between the SAF and the STC; 25.4 $DW mg m^{-3}$ (6.9–82.8) for the STC and 7.98 $DW mg m^{-3}$ (1.2–18.4) north of the STC. In the Indian sector of the Sub-Antarctic, ealier summer records North of Kerguelen Islands, showed values of 43.3 $DW mg m^{-3}$ for a 100 m water column, while biomass north of 45°S was around 8 $DW mg m^{-3}$ (Razouls and Razouls, 1982).

Mesoscale description of zooplankton communities have always been a problem with net sampling, which provides only snapshots of the population structure and leaves open the question of how to integrate larger scale features. The OPC appears to give an interesting answer, which showed a fair agreement with traditional sampling and illustrates in a quantitative way 2D spatial heterogeneity in both size structure and biomass.

Acknowledgements

This work was supported by the "Institut National des Sciences de l'Univers" and the French Joint Global Ocean Flux Study program. The authors are indebted to the "Institut Français de Recherche et Technologie Polaire", which made the *ANTARES* program possible through the use of the R.V. *Marion Dufresne*, and to the officers and crew. The authors also wish to acknowledge their colleagues, in particular Dominique Tailliez and Bernard Olivier, for technical help.

References

Barange, M., Pakhomov, E.A., Perissinotto, R., Froneman, P.W., Verheye, H.M., Taunton-Clark, J., Lucas, M.I., 1998. Pelagic community structure of the subtropical convergence region south of Africa and in the mid-Atlantic Ocean. Deep-Sea Research I 45, 1663–1687.

Currie, W.J.S., Claereboudt, M.R., Roff, J.C., 1998. Gaps and patches in the ocean: a one-dimensional analysis of planktonic distributions. Marine Ecological Progress Series 171, 15–21.

Grachev, D.G., 1991. Frontal zone influences on the distribution of different zooplankton groups in the central part Indian sector of the Southern Ocean. In: Samoila, M.S., Shumkova, S.O. (Eds.), Ecology of Commercial Marine Hydrobionts. TINRO Press, Vladivostok, pp. 19–21. (in Russian).

Grant, S., Ward, P., Murphy, E., Bone, D., Abott, S., 2000. Field comparison of an LHPR net sampling system and an optical plankton counter (OPC) in the Southern Ocean. Journal of Plankton Research 22, 619–638.

Heath, M.R., Dunn, J., Fraser, J.G., Hay, S.J., Madden, H., 1999. Field calibration of the optical plankton counter with respect to *Calanus finmarchicus*. Fisheries and Oceanography 8 (Suppl. 1), 13–24.

Herman, A.W., 1988. Simultaneaous measurement of zooplankton and light attenuance with a new optical plankton counter. Continental Shelf Research 8, 205–221.

Herman, A.W., 1992. Design and calibration of a new optical plankton counter capable of sizing small zooplankton. Deep-Sea Research I 39, 395–415.

Herman, A.W., Cochrane, N.A., Sameoto, D.D., 1993. Detection and abundance estimation of euphausiids using an optical plankton counter. Marine Ecological Progress Series 94, 165–173.

Huntley, M.E., Zhou, M., Nordhausen, W., 1995. Mesoscale distribution of zooplankton in the California current in late spring, observed by optical plankton counter. Journal of Marine Research 53, 647–674.

Huntley, M.E., González, A., Zhu, Y., Zhou, M., Irigoyen, X., 2000. Zooplankton dynamics in a mesoscale eddy-jet system off California. Marine Ecological Progress Series 201, 165–178.

Kato, S., Ito, N., Gunji, K., Aoki, I., Nishida, S., 1997. Small- and Mesoscale zooplankton distributions in the Kuroshio Area. JAMSTECR 36, 129–136.

Mullin, M.M., Cass-Calay, S.L., 1997. Vertical distributions of zooplankton and larvae of the Pacific hake (whiting), *Merluccius productus*, in the California current system. CalcCOFI Report 38, 127–136.

Nagata, Y., Michida, Y., Umimura, Y., 1988. Variation of positions and structures of the oceanics fronts in the Indian Ocean sector of the Southern Ocean in the period from 1965–1987. In: Sahrhage, D. (Ed.), Antarctic Ocean and Resources Variability. Springer, Berlin, pp. 92–98.

Osgood, K.E., Checkley Jr., D.M., 1997. Observations of deep aggregations of *Calanus pacificus* in the Santa Barbara Basin. Limnology and Oceanography 42, 997–1001.

Pakhomov, E.A., Perissinotto, R., McQuaid, C.D., Froneman, P.W., 2000. Zooplankton structure and grazing in the Atlantic sector of the Southern Ocean in late austral summer 1993. Part 1. Ecological zonation. Deep-Sea Research I 47, 1663–1686.

Park, Y-H., Gamberoni, L., 1997. Cross-frontal exchange of Antartic intermediate water and Antartic bottom water in the Crozet Basin. Deep-Sea Research II 44, 963–986.

Razouls, C., 1995. Diversité et répartition géographique chez les copépodes pélagiques. 1-Calanoida. Annales de l'Institut océanographique N.S 71, 81–404.

Razouls, C., 1996. Diversité et répartition géographique chez les copépodes pélagiques 2-Platycopioida, Misophrioida, Mormonilloida, Cyclopoida, Poecilostomatoida, Siphonostomatoida, Harpacticoida, Monstrilloida. Annales de l'Institut océanographique N. S. 72 (1), 1–14.

Razouls, C., Razouls, S., 1982. Element du bilan energétique du mesozooplancton antarctique. CNFRA 53, 131–141.

Sameoto, D., Cochrane, N., Herman, A., 1990. Use of multiple frequency acoustics and other methods in estimating copepod and euphausiid abundances. ICES, CM 1990/L:81, pp. 1–9.

Sheldon, R.W., Prakash, A., Sutcliffe Jr., W.H., 1972. The size distribution of particles in the ocean. Limnology and Oceanography 17, 327–340.

Sprules, W.G., Jin, E.H., Herman, A.W., Stockwell, J.D., 1998. Calibration of an optical plankton counter for use in freshwater. Limnology and Oceanography 43, 726–733.

Stockwell, J.D., Sprules, J.D., 1995. Spatial and temporal patterns of zooplankton biomass in Lake Erie. ICES Journal of Marine Science 52, 557–567.

Vidal, J., Whitledge, T.E., 1982. Rates of metabolism of planktonic crustaceans as related to body weight and temperature of habitat. Journal of Plankton Research 4, 77–84.

Wieland, K., Petersen, D., Schnack, D., 1997. Estimates of zooplankton abundance and size distribution wih the optical plankton counter (OPC). Archives of Fisheries and Marine Research 45, 271–280.